Turbulent Flow Studies in Two Arc-Heated Duct Facilities

M. ALAN COVINGTON* AND NICK S. VOJVODICH†
NASA Ames Research Center, Moffett Field, Calif.

The results of preliminary investigation of the flow conditions in two arc-heated duct facilities are presented. These facilities were developed to simulate space shuttle vehicle entry conditions by providing high-temperature, supersonic, turbulent boundary-layer flows over relatively large samples of candidate materials for thermal protection systems. In one facility, a rectangular duct provides two-dimensional flow over a flat plate model, whereas in the other facility a contoured nozzle provides axisymmetric flow through a hollow circular cylinder of test material. Convective heating rate measurements are compared to theory and other experimental data and, with Teflon ablation measurements, are used to verify turbulent flow in both facilities. The ranges of heat-transfer rate, heat-transfer coefficient, and surface temperature attained are shown to provide adequate simulation of the space shuttle entry heating environment.

Nomenclature

A^* = nozzle throat cross-sectional area
C_{fo} = skin-friction coefficient
d^* = nozzle throat diameter
H = enthalpy
H_{eff} = effective heat of ablation
ΔH = $H_t - H_w$
L = length
L/D = lift to drag ratio
Le = Lewis number
M = Mach number
$\dot{m},\dot{m}_w$ = mass flow rate and surface mass loss rate
p = pressure
Pr = Prandtl number
$\dot{q}$ = heat-transfer rate
r = radius
Re = Reynolds number
St = Stanton number
T = temperature
t = thickness
u = velocity
w = width
x,y = streamwise and cross-stream distance
$z,\dot{z}$ = surface normal distance and recession rate
ε = emissivity
ρ = density
σ = Stefan-Boltzmann constant

Subscripts

c = chamber
$\mathcal{C}_L$ = centerline
cw = cold wall
e = boundary-layer edge
h = hydraulic radius
hw = hot wall
L = unit length
mc = mixing chamber
t = total
w = wall

Introduction

THE aerothermodynamic entry conditions associated with the space shuttle orbiter vehicles present new facility requirements for adequate simulation of the convective heating environment. Most existing arc-heated wind-tunnel facilities were originally designed for study of the ballistic entry problem and allow only laminar flow, stagnation point testing of relatively small models.[1] However, meaningful tests of candidate materials for orbiter re-entry thermal protection systems (TPS) will require facilities for testing much larger samples in a turbulent boundary layer over ranges of convective heating parameters appropriate to the space shuttle vehicle (SSV) entry.

Although considerable effort will be made to shape both the entry trajectory and vehicle surface contour to provide the maximum amount of laminar flow with attendant lower surface heat transfer,[2] several factors including large vehicle size, surface roughness, and anticipated cross-range requirements indicate that a large fraction of the vehicle may be exposed to a turbulent boundary layer with its higher heat-transfer rates. Conservative design of a full-scale thermal protection system will therefore require assessing the effects of turbulent flow on the ablative and thermal behaviour of candidate TPS materials, the thermostructural response of reasonably sized panels of these materials, and the problems of joints and fasteners associated with large panels.

To provide appropriate flow and heating environments for testing proposed TPS materials, two duct facilities have been constructed at the Ames Research Center. This paper: 1) describes these two facilities that are currently used to test relatively large samples for long times in a high temperature, supersonic, turbulent boundary layer; 2) presents stream calibration measurements for these facilities; and 3) compares the facility convective heating conditions with those expected during space shuttle orbiter vehicle entry.

Description of Facilities

The rectangular duct shown in Fig. 1 consists of three separate water-cooled sections that provide two-dimensional flow over a flat test area. A transition section changes the flow channel from a circular cross section (2 in. inner diameter) at the arc heater outlet to a square cross section (1 in. by 1 in.) at the nozzle section inlet. The nozzle section symmetrically expands the flow in the horizontal plane about the duct axial centerline while the vertical dimension of the channel is held constant. The nozzle throat dimensions are 0.5 in. wide and 1 in. high; the exit dimensions are 5 in. wide and 1 in. high. The nominal exit Mach number is 3.4. The nozzle section is connected to a test section having a constant height and width of 1 in. and 5 in., respectively, throughout its length. The gas stream passes through a short length (10 in.) of this test section before flowing over a 4 in. wide by 6 in. long test area in the bottom wall. The test section is constructed so that either a flat plate material sample or a water-cooled flat plate can be installed in the test area to form part of the lower duct wall.

Presented as Paper 71-262 at the AIAA 6th Aerodynamic Testing Conference, Albuquerque, N. Mex., March 10–12, 1971; submitted April 7, 1971; revision received January 26, 1972.
Index categories: Boundary Layers and Convective Heat Transfer—Turbulent; Supersonic and Hypersonic Flow; Material Ablation.
* Research Scientist. Member AIAA.
† Research Scientist.

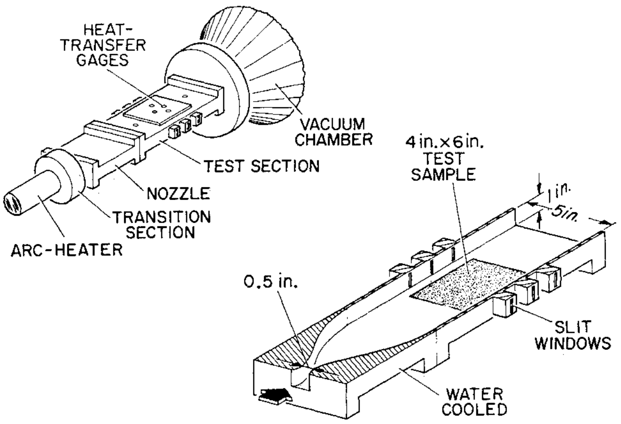

Fig. 1 Rectangular turbulent flow duct.

After passing through the duct the gas stream is directed through a diffuser into a high capacity, 5-stage, steam ejector vacuum system.

Ports are provided on the upper wall of the test section for installation of sensors to measure wall pressures and heat-transfer rates. Static pressure can be measured at centerline and two off-centerline stations; heating rate can be measured at five centerline and two off-centerline locations. Pressures are measured with variable capacitance diaphragm-type cells; heat-transfer rates are measured with water-cooled steady-state calorimeters. The calorimeters above the test area can be replaced by window inserts to permit measurement of model surface temperature. Six slit windows are located in the duct sidewalls (see Fig. 1) to allow optical measurements of the boundary layer or model.

Testing material samples in the rectangular duct presents a problem in that no means is provided for protecting the sample from the stream during arc heater start-up as is done in conventional arc tests. Special fast start procedures are employed to establish steady-state flow conditions as quickly as possible to minimize the time the sample is exposed to transient steam conditions. It was found that steady conditions could be attained consistently in 10 sec or less, minimizing the effects of start-up transients on over-all material response for typical test times of 1 min to 0.5 hr.

In the axisymmetric duct shown in Fig. 2 an arc-heated gas stream flowing through a contoured, axisymmetric, water-cooled nozzle is directed through a hollow circular tube made of the material to be tested. This nozzle has a throat diameter of 0.75 in., an exit diameter of 2 in., and a nominal exit Mach number of 3.1. After passing through the tube, the gas stream is discharged into a 5-stage steam ejector vacuum system. During arc heater start-up the test sample tube is held in the retracted position shown in Fig. 2 and, after steady flow is established, radial surveys of stream properties are made in a plane 1 in. downstream and parallel to the nozzle exit plane. After completion of the stream surveys, the tubular model is swung into the test stream so that the

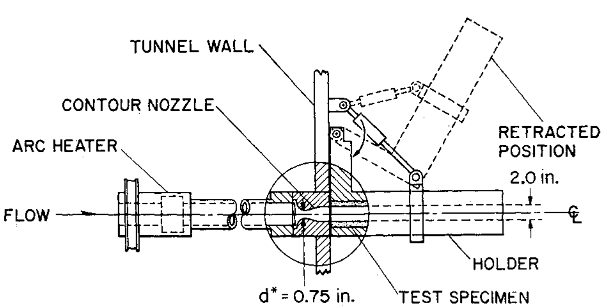

Fig. 2 Axisymmetric turbulent flow duct.

Table 1 Facility operating conditions

	Axisymmetric duct	Rectangular duct
Power input, Mw	0.54–3.8	0.4–2.7
Chamber pressure, atm	3.7–55.0	3.3–52.0
Wall pressure, atm	0.032–0.88	0.040–0.30
Heating rate (cold wall), Btu/ft^2-sec	20–120	12–100
Unit Reynolds number, ft^{-1}	$0.15–3.3 \times 10^6$	$0.0078–4.1 \times 10^6$
Nozzle area ratio	7.1	10
Mach number	3.1	3.4

upstream end of the model fits over the contoured nozzle exit (Fig. 2).

By virtue of its higher mass flow rate per unit flow cross-sectional area, the axisymmetric duct was capable of testing at higher Reynolds numbers and, because of its internal geometry, at higher surface temperatures than attainable on flat plate models in the rectangular duct. However, the inherent disadvantages of pipe flow tests characteristic of the axisymmetric duct are well known and include the difficulties of making radiation measurements on the internal hot surface and nonuniform heating along the tube as well as requiring excessive amounts of material for models. These limitations make the rectangular duct more attractive for most TPS studies.

A high-temperature gas stream for each facility was generated by a Linde N-4000 high pressure arc heater.[3] Table 1 shows the range of operating conditions that have been attained in the two facilities. Both air and nitrogen can be used as test gases. A few tests were made in the rectangular duct with a mixing chamber installed between the arc heater and the nozzle section so that additional unheated air could be injected to increase the total mass flow rate with an attendant decrease in total enthalpy. This allowed definition of the duct operating characteristics at higher pressures and Reynolds numbers than could be attained with flow through the arc heater only.

The nozzle throat air mass flow rate and total enthalpy as a function of arc chamber pressure for the two facilities are

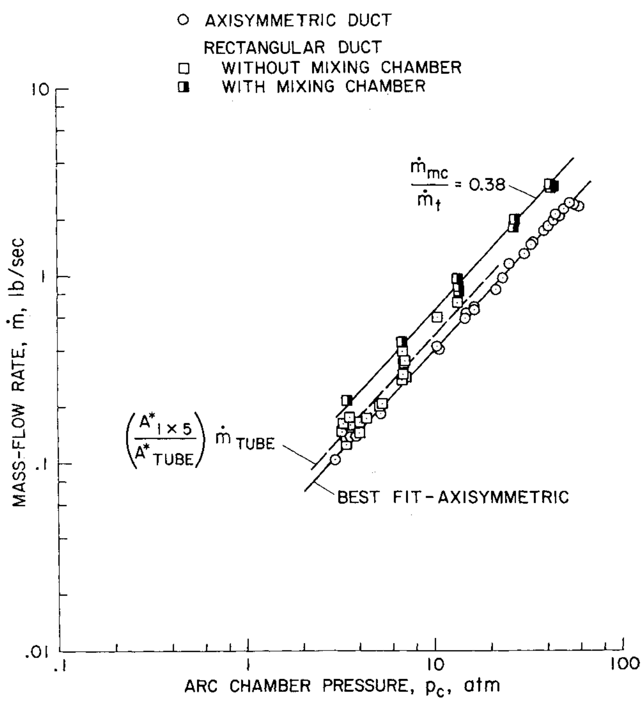

Fig. 3a Mass flow variation with arc chamber pressure.

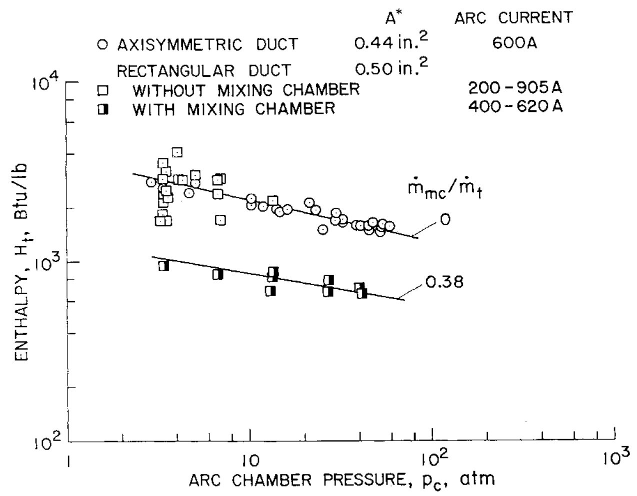

Fig. 3b Enthalpy variation with arc chamber pressure.

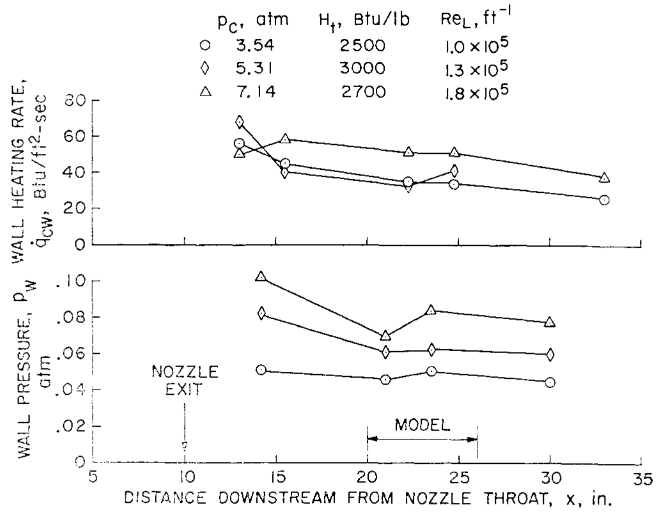

Fig. 4 Centerline wall heating rate and pressure distribution in rectangular duct.

shown in Fig. 3. As is done throughout this paper, total enthalpy has been calculated by the equilibrium sonic flow method[4] using the measured mass flow rate and chamber pressure. This calculation procedure yields bulk total enthalpy values that should be valid at the nozzle throat but are high after the stream is expanded. The differences in mass flow, and resulting differences in total enthalpy levels, are due mainly to the differences in nozzle throat area between the rectangular and axisymmetric ducts (0.5 and 0.44 in.^{2}, respectively). The scatter in the total enthalpy (Fig. 3b) at low chamber pressures is due to uncertainties in mass flow rate measurements at low flow rates as indicated in Fig. 3a.

Duct Flow Characteristics

The initial calibration tests were conducted primarily to characterize the nature of the flow within the test region of each duct. To simulate SSV entry conditions and conduct meaningful tests of candidate TPS materials, it was important to know the level and distribution of heating rate and pressure to determine if turbulent flow existed over the measured ranges of heating parameters. The most direct and readily available method of accomplishing this was to measure the convective cold wall heating rate and compare both the level and pressure dependence of the results with laminar and turbulent theories.

Flow Measurements

Typical variations of rectangular duct wall pressure and cold wall heating rate measurements taken in the test section are presented in Fig. 4 for three different chamber pressures and enthalpies. It can be seen that the pressure field through the duct becomes increasingly nonuniform as pressure is increased but that the heating rate distribution does not reflect the changes in local pressure level. This may be explained by the influence of a thick boundary layer at lower pressures and higher enthalpies. The variation in heating rate at the point nearest the nozzle exit ($x = 13$ in.) is possibly caused by shifts in the wave angle of disturbances originating in the nozzle section. The data shown suggest that these shifts are a function of both enthalpy and pressure.

The effect of boundary-layer thickness on the coupling of heat transfer and pressure waves has been noted by others.[5,6] In particular, a thick, supersonic turbulent boundary layer has been observed to obscure the wall effects of flow field disturbances, and is thought to be due to viscous diffusion of pressure waves within the boundary layer. Such a mechanism would explain the features in Fig. 4.

For the axisymmetric duct the wall heat-transfer rate was determined from in-depth temperature rise measurements in graphite tubes. The measurement station was 11.5 in. from the exit of the contoured nozzle. In determining the heating rate a correction was made for the heat capacity of the metal support structure holding the tube.

In addition, radial surveys of Pitot pressure and stagnation heating rate were made in the stream produced by the contoured nozzle of the axisymmetric duct facility. The rapid response instrumentation consisted of a 0.625 in. diam water-cooled pressure probe with an orifice diameter of 0.125 in., and a commercially available 0.625 in. diam steady-state heat-transfer gage with a sensing diam of 0.05 in. The measurements were conducted over an arc chamber pressure range of 5 to 53 atm. The results of two of the surveys are shown in Fig. 5. In all cases the test chamber pressure was considerably lower than the nozzle exit static pressure so that the flow was highly overexpanded. This can be noted by the rapid drop in pressure that occurs at $r/r_{exit} = 0.5$, which approximately corresponds to the location associated with the limiting angle of the expansion fan for a Mach number of 3.1. The flow in the internal region ($0 \leq r/r_{exit} \leq 0.5$) can be considered to be representative of the flow existing in the interior of hollow, cylindrical tube models. The heat-transfer distribution in this core region is shown to be relatively insensitive to both arc chamber pressure and radial position.

By combining the measured pressure and heat transfer distribution data the enthalpy profile may be calculated from the Fay-Riddell scaling law for stagnation region heating, i.e., $H/H_{\mathbb{C}} = \dot{q}(p)^{-1/2}/[\dot{q}(p)^{-1/2}]_{\mathbb{C}}$. The results of these calculations (Fig. 5) demonstrate a rather weak dependence of enthalpy and, hence, velocity upon total pressure. This is particularly true when compared to similar results obtained in surveys of low pressure, high enthalpy laminar flow streams.[1] This difference in radial dependence of enthalpy suggests that the flow in the present tests may be turbulent at the measurement station. Indeed, it has been suggested that the flow leaving the arc heater itself may be turbulent because the stabilizing magnetic field superimposes a rotational velocity component on the mean axial velocity vector, resulting in intense mixing in the arc chamber.

Comparison of Heat-Transfer Data with Theory

In the rectangular duct the axial pressure gradient may be small enough and the duct width to height ratio large enough that flow in the test section can be approximated by an appropriate theory for a supersonic, compressible, dissociated,

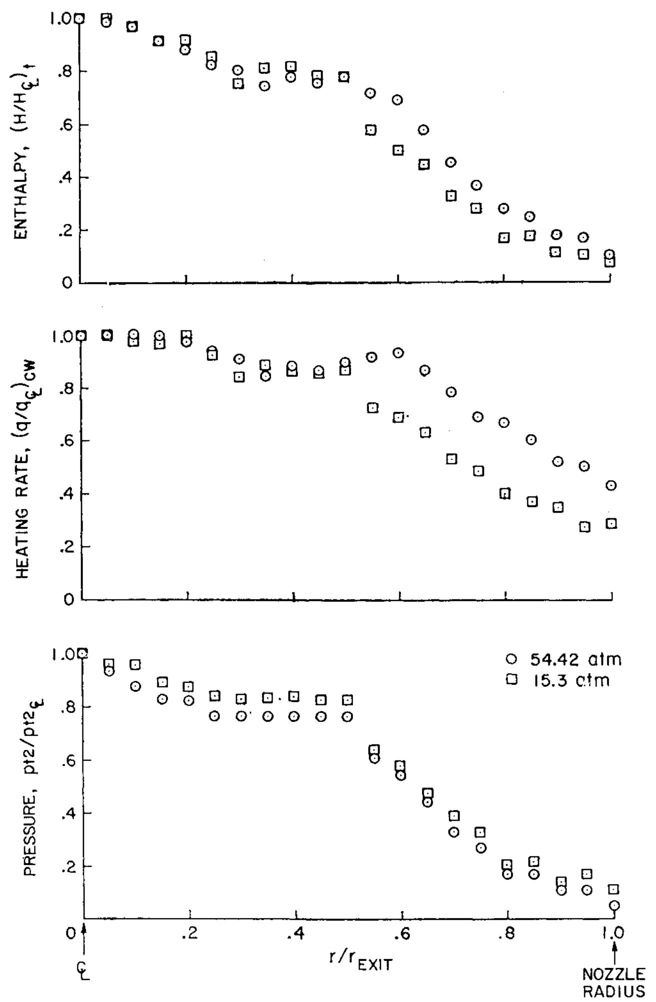

Fig. 5 Radial surveys of Pitot pressure, convective heating rate, and enthalpy in axisymmetric duct.

turbulent boundary layer over a flat plate. The heat transfer rate in the absence of ablation can be written as[7]

$$\dot{q}_{cw} = \rho_e u_e Pr^{-2/3}(C_{f0}/2)(H_t - H_w) \tag{1}$$

where

$$C_{f0} = C_{f0}(Re, M, T_e/T_w)$$

and the dissociation terms appearing in Eqs. (7–89) of Ref. 7 are neglected because, for the low enthalpies considered in these duct flows, the dissociation is negligible. By further noting that C_{f0} is relatively insensitive to the wall-to-edge temperature ratio for small values of T_w/T_e, and by assuming a boundary-layer edge Mach number of 3.5 as typical for the ducts, the skin friction coefficient can be approximated by

$$C_{f0} = 0.0328\ Re^{-0.12} \tag{2}$$

For laminar flow over a flat plate, the skin-friction coefficient can be expressed as

$$C_{f0} = 0.664\ Re^{-0.5} \tag{3}$$

In Fig. 6 the theoretical dependence of cold wall heat transfer upon both pressure and enthalpy as predicted by Eq. (1) using the approximation given by Eq. (2) for turbulent flow is shown as is laminar flow theory using Eqs. (3) and (1). Since mass flow rate through a given nozzle is proportional to arc heater chamber pressure at a fixed value of enthalpy, duct Reynolds number is proportional to chamber pressure to a good approximation. Note that a Reynolds number based on a flow length of 1 ft was used in calculations appearing in Fig. 6.

Also shown in Fig. 6 are heat-transfer data from operation of both the rectangular and axisymmetric ducts obtained over

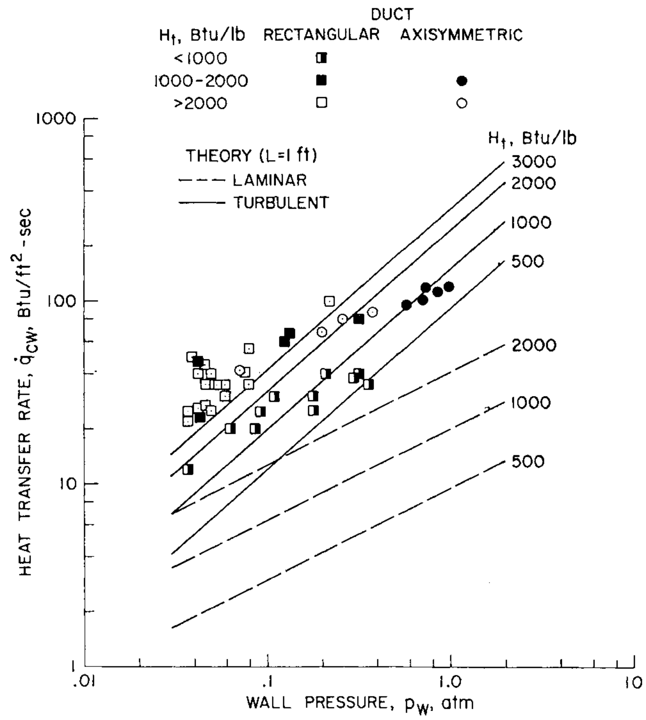

Fig. 6 Comparison of measured duct heat transfer with flat plate theory.

ranges of enthalpy and pressure. The cold wall heating rate and wall pressure shown for the rectangular duct are average values measured by instrumentation located opposite the 4 by 6 in. test area in the test section, while the axisymmetric duct the cold wall heating rate is that calculated from the graphite tube temperature rise measurements with the wall pressure assumed to be the theoretical static pressure at the nozzle exit for an area ratio of 3.1. Both the magnitude and trend of heating rate indicate that the flow in both facilities is turbulent and there is reasonable agreement with turbulent theory.

A comparison was also made with available internal channel flow data and theory. However, most experimental studies of fluid flow in internal passages have been confined to low speeds and low levels of stream temperature. An example of the large body of information developed for this classical problem is the study of Hartnett et al.[8] who investigated the influence of rectangular duct aspect ratio on the Reynolds number dependence of the skin friction coefficient for fully developed flows. They found that the transition criterion of a Reynolds number (based on hydraulic radius) of 3500 was the same for both circular configurations and all rectangular ducts with aspect (width/height) ratios equal to or greater than 5. To compare the present high temperature, compressible flow results with those of Ref. 8 as well as with the experiments and theory of Gaudette et al.,[9] the heat-transfer data obtained in both the axisymmetric and rectangular ducts have been presented in Fig. 7 in nondimensional Stanton number form as a function of Reynolds number. The data of Gaudette et al. were measured on the wall of a rectangular duct with an aspect ratio of 4 and an arc-heated, supersonic ($M = 2.5$) flow. The stream total enthalpies (1600–3230 Btu/lb) provided by the Boeing facility were comparable to those of the present investigation, but the peak of the mass flow rates (0.06–0.125 lb/sec) was about an order-of-magnitude lower than the maximum of the present flow rates (0.1–3.0 lb/sec) resulting in the lower Reynolds numbers for their experiments. In the range of Reynolds numbers common to both facilities the present results exhibit a considerable degree of scatter due mainly to the corresponding uncertainty in the enthalpy [see Fig. 3b], which enters into the denominator of the Stanton number equation. However, at Reynolds numbers com-

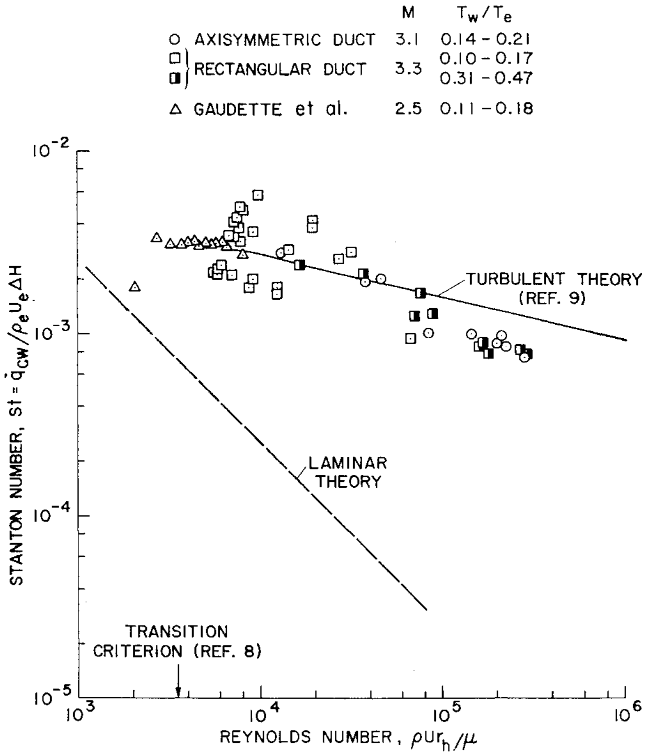

Fig. 7 Comparison of measured Stanton number with internal flow theory.

parable to those of the Boeing tests the mean of the present data agrees favorably with their heat-transfer results. Furthermore, the results from the axisymmetric and rectangular ducts agree well and, if we assume that $Le = Pr = 1.0$, this finding for the two dissimilar internal geometries is in accordance with the results of Hartnett et al.[8] discussed above.

Also shown on Fig. 7 are the theoretical predictions of Ref. 9 for both fully developed laminar and turbulent flow of a compressible gas in an internal channel. Comparison of the axisymmetric and rectangular duct heat-transfer data with these theories shows a trend with Reynolds number that agrees favorably with the turbulent theory and levels that are a factor of 10 to 19 times higher than the laminar theory. Both of these observations indicate that the flows in these facilities are turbulent. Some of the noted differences between the results and the turbulent theory of Ref. 9 can be attributed to such effects as the influence of Mach number and wall temperature ratio on the heating calculations; however, the data are not considered to be of sufficient quality to make any conclusions regarding these effects.

Teflon Ablation Measurements

Ablation tests of Teflon were included as part of the initial calibration effort in both facilities to obtain further information on the nature of the boundary-layer flows within the ducts. Teflon is a material whose response has been well characterized for laminar flows[1,10–13] and, to a lesser extent, for turbulent flows.[6,13–15] As pointed out in Refs. 6, 13, and 17, crosshatch patterns formed on ablating Teflon surfaces can be used to demonstrate supersonic turbulent boundary-layer flow. Two motivations for testing Teflon were to use this phenomenon to verify turbulent flow conditions and to investigate wall heat-transfer distributions in the ducts.

The Teflon models tested in the two-dimensional rectangular duct were configured as shown in Fig. 8. The exposed upper surface of the model had planform dimensions of 4 in. in width and 6 in. in length to correspond to the test area in the bottom wall of the duct. The model was 1 in. thick. The

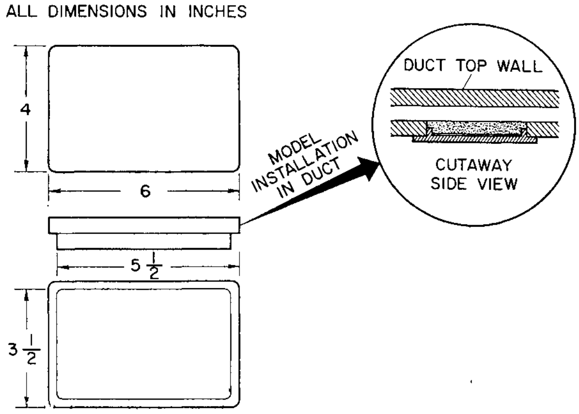

Fig. 8 Rectangular duct Teflon model design.

models were held in an uncooled model holder by small screws penetrating the sides. This model holder, in turn, was mounted in the bottom of the duct. Care was taken during installation to prevent steps between the bottom wall of the duct and the leading and trailing edges of the model.

Models for the axisymmetric duct facility are hollow right circular cylinder tubes having an inside diam. of 2 in. to match the contoured nozzle exit dimension. Teflon tubes of 24 in. length and 0.5 in. wall thickness have been tested, while graphite tubes of 12 in. length and 0.5 in. wall thickness were used for measurement of the wall heat transfer as previously described.

Teflon tubes tested in the axisymmetric duct facility exhibited characteristic crosshatched patterns with ordered criss-cross grooving; their existence gives good evidence of turbulent flow.[6,13,16,17] The halves of two tubes cut lengthwise after exposure are shown in Fig. 9. The tube on the top was run in nitrogen and the tube on the bottom was run in air for the same exposure time at the same nominal heating and flow conditions. In both air and nitrogen tests in the axisymmetric duct, a liquid melt layer was observed to flow along the ablating surface and to form droplets at the end of the tube that were subsequently entrained in the exiting gas stream.

Teflon models tested in the rectangular duct did not show the same surface patterns as the tubes. Rather, a series of longitudinal grooves or striations were observed on the forward portion of several models tested at low wall pressure (low Reynolds number) conditions. Such streamwise grooving has been observed previously during ablation in supersonic streams.[6,13,16,17]

The use of Teflon models can also furnish information on local heat-transfer distributions over the model surface. For an ablator such as Teflon, the mass loss under steady ablation conditions can be related to the heating rate by[10]

$$\dot{q}_w = H_{eff}\dot{m}_w = H_{eff}\rho_w\dot{z}_w$$

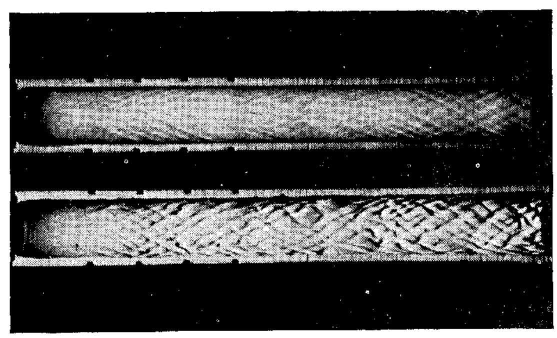

Fig. 9 Cross-hatching patterns on Teflon tube models.

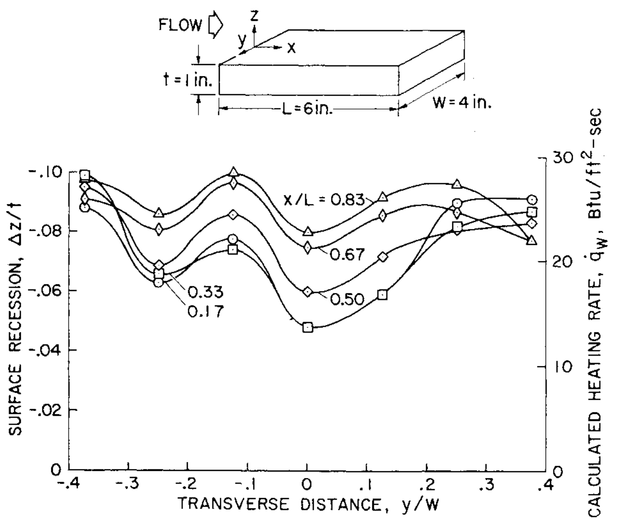

Fig. 10 Surface recession and heating rate distributions on Teflon model.

The effective heat of ablation for a turbulent boundary layer can be assumed constant to a first approximation.[14,15] Measurements of local surface recession can therefore be used to provide a detailed mapping of the relative imposed heat-transfer rate over the model so long as the ablating surface itself does not introduce any disturbances into the gas stream.

Measured surface recession distribution on a 1 in. thick Teflon model tested in the rectangular duct is shown in Fig. 10. For this model, the stream enthalpy was 2600 Btu/lb, pressure was 0.045 atm, and exposure time was 60 sec. The effects of uneven ablation caused by stream nonuniformities can be seen. Also, surface recession generally increases in the streamwise direction except in local areas of higher heating. Local wall heat-transfer rates derived from the measured mass loss are also presented in Fig. 10 assuming an effective heat of ablation of 1500 Btu/lb.[15] There can be as high as 35% variation in local heating rate across the model at a given streamwise station although the average variation is less. Heating rates near the rear of the model are 15 to 40% higher than near the front. The general level of heat-transfer rates derived from these surface recession data agrees well with turbulent boundary-layer heating rates expected for these stream conditions (e.g., Fig. 6) in spite of the lack of criss-cross surface grooving such as was formed in the cylindrical Teflon tubes.

Although the variations of cold wall heating rate over the rectangular duct test area are quite large, tests on typical TPS materials indicate that meaningful results can be obtained in this facility. Tests[18] on a typical charring ablator have shown that there are only slight lateral and longitudinal variations of degradation and surface recession of exposed samples. This is attributed to the high thermal conductivity of the char causing a "smearing" of local heating rate variations. Recent tests on rigidized ceramic fiber (so-called surface insulator) materials have shown that the surface temperature gradients induced by nonuniform local heating rates in the duct are acceptable for evaluation of these types of low thermal conductivity materials with their low-strength coatings. In contrast, preliminary tests of one thin metal panel indicated that the local heat-transfer nonuniformities as well as inadequate panel design contributed to the buckling that was experienced. It should be pointed out that even in the absence of flowfield disturbances in the duct, any uncooled model surface mounted in the duct wall will experience nonuniform streamwise heating due to the temperature discontinuity between the cooled duct wall and the hot model surface. This problem will be inherent in any internal duct having high temperature gas flow and highly cooled walls.

Requirements for Simulation of SSV Entry Environment

To assess the degree of simulation afforded by the two facilities, consider the range of heating environment variables expected for various space shuttle configurations and rank them in terms of importance with regard to the study of thermal protection system response. There is currently a wide possibility of flight configurations and attendant trajectories. However, they can be broadly divided into two classes: 1) the low crossrange, low L/D type with characteristic heating times of 500 sec, and 2) the high crossrange, high L/D type with characteristic heating times of 2000 sec. The heat-transfer parameters vary not only with respect to entry time, but also with position on the vehicle. Attention will be focused on the turbulent heating that is expected on the windward body of these two classes of configurations since these areas will make up a sizable fraction of the total vehicle area and, accordingly, will require a large percentage of the heat shield weight. The high heating rate areas such as nose caps, and wing and fin leading edges are responsible for only a small fraction of the TPS weight, and the laminar conditions characteristic of these locations are readily duplicated in other existing small scale, low power arc-heated facilities.

Table 2 contrasts the turbulent heating conditions expected on the lower surface of the two classes of vehicles and compares them with the conditions measured in the 1 by 5 in. rectangular duct facility. The primary simulation variable, the level of hot wall heat-transfer rate, and the associated temperature (for an assumed emissivity of 0.8) are comparable for both entry modes and the range is duplicated satisfactorily by the test facility. The enthalpy for flight varies between 5000 and 12000 Btu/lb during periods of significant heating. These values are considerably higher than those attainable with the N-4000 heater used in the present study. However, a higher enthalpy heater that has been subsequently coupled with the rectangular duct provides better enthalpy simulation.

Table 2 Comparison of space shuttle thermal environment with facility capability

	Flight		Test
Parameter	High crossrange	Low crossrange	Rectangular duct
Heating rate (hot wall) $\dot{q}_{hw}$, Btu/ft^2-sec	9–29	5–21	4–38
Total enthalpy H_t, Btu/lb	$5–12 \times 10^3$	$5–11.5 \times 10^3$	$0.7–3.9 \times 10^3$
Wall temperature $(\varepsilon = 0.8) T_w$, °F	$1.8–2.5 \times 10^3$	$1.5–2.25 \times 10^3$	$1.33–2.74 \times 10^3$
Heat-transfer coefficient $C_h = \dot{q}_{hw}/\Delta H$ lb/ft^2-sec	$0.8–6.9 \times 10^{-3}$	$0.4–4.8 \times 10^{-3}$	$6–60 \times 10^{-3}$
Wall pressure p_w, atm	$0.14–0.28 \times 10^{-2}$	$0.6–2.7 \times 10^{-2}$	$4–30 \times 10^{-2}$

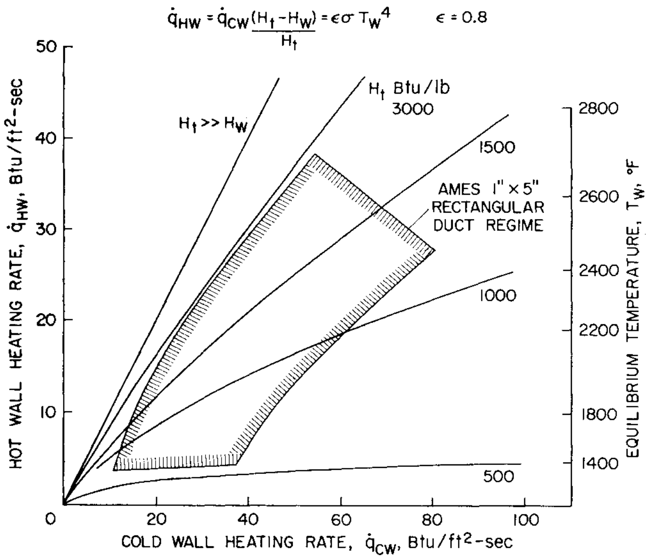

Fig. 11 Influence of steam enthalpy on hot wall heating rate and equilibrium temperature.

The enthalpy level (Fig. 11) of the stream plays a strong role in determining both the hot wall heating rate and radiation equilibrium temperature, accounting for the differences between the tabulated hot wall heating rates and the cold wall values shown in Fig. 6. The enthalpy level also controls the extent of boundary-layer dissociation and thereby the influence of TPS surface catalytic effects. These effects may be of particular importance for the high cross-range vehicle, and are not simulated adequately in the relatively low enthalpy test stream produced by the N-4000 heater. Furthermore, the enthalpy in combination with the heat-transfer level determines the heat-transfer coefficient, a parameter that Goldstein[19] has shown to be important in the analysis and interpretation of data obtained on the surface oxidation of metallic heat shield candidates such as thoria-dispersed nickel-chrome alloy. In both respects, the lower enthalpy tests may be considered conservative. The wall pressure is the one factor, apart from heating time, that differs appreciably for the two entry classes, being an order-of-magnitude higher for low cross-range vehicles. The test values are higher than the levels expected for both classes. The wall pressure will act primarily as a boundary loading condition and, as such, will influence the thermo-structural response due to the coupling between the external aerodynamic forces and the thermal deformation of candidate heat shields. Simulation will therefore only be required for the study of interaction heating problems associated with large panel testing.

In summary, it has been demonstrated that the high temperature supersonic boundary-layer environment provided by the rectangular duct facility provides adequate simulation of the significant flight heating factors and, in the cases where a one-to-one correspondence between flight and test does not exist, the test values are conservative.

Conclusions

Two arc-heated duct facilities have been developed to provide a continuous supersonic, high temperature, turbulent boundary-layer flow for evaluating large samples of candidate thermal protection materials for the space shuttle vehicle. The facilities are a 1 by 5 in. rectangular duct that provides for tests of 4 by 6 in. flat samples, and a 2 in. i.d. axisymmetric duct that is used for tests of hollow tubes up to 24 in. long.

The level and trend of experimental heat-transfer data obtained in both facilities are in fair agreement with flat plate turbulent boundary-layer theory, and in good agreement with internal turbulent flow theory and experiment. Tests of Teflon samples and the interpretation of resulting ablation surface patterns provide further evidence of turbulent flow as well as a detailed mapping of relative heat-transfer distributions over the sample surface.

Test conditions in the rectangular duct provide adequate simulation of the heating rate, heat-transfer coefficient, and surface temperature expected during both low and high cross-range atmospheric entries of space shuttle vehicles. The duct test conditions are conservative for the entry heating parameters of enthalpy and pressure that are not well simulated.

References

[1] Hiester, N. K., Clark, C. F., and Vojvodich, N. S., "Ablative Characterization of Seven Heat Shield Materials—A Review of the NASA-SRI Round Robin Program," *Proceedings of the AIAA/ASME 10th Structures, Structural Dynamics, and Materials Conference*, American Society of Mechanical Engineers, April 1962, pp. 57–68.

[2] Lecat, R., "Reentry: A New Ball Game," *Space/Aeronautics*, Feb. 1970, pp. 39–45.

[3] Brown, S. A., and Patton, J. B., "Calibration and Operation of the Linde N-4000 Arc Heater With 1/2 and 3/8 Inch Diameter Constrictors," AEDC TR-65-102, June 1965, Arnold Engineering Development Center, Arnold Air Force Station, Tullahoma, Tenn.

[4] Winovich, W , "On the Equilibrium Sonic-Flow Method for Evaluating Electric-Arc Air Heater Performance," TN D-2132, 1964, NASA.

[5] Larson, H. K. and Mateer, G. G., "Cross-Hatching-A Coupling of Gas Dynamics With the Ablation Process," AIAA Paper 68-670, Los Angeles, Calif., 1968.

[6] Natchsheim, P. R. and Larson, H. K., "Crosshatched Abaltion Patterns in Teflon," AIAA Paper 70-769, Los Angeles, Calif., 1970.

[7] Dorrance, W. H., *Viscous Hypersonic Flow*, McGraw-Hill, New York, 1962.

[8] Hartnett, J. P., Koh, J. C. Y., and McComas, S. T., "A Comparison of Predicted and Measured Friction Factors for Turbulent Flow Through Rectangular Ducts," *Transactions of the ASME: Journal of Heat Transfer*, Feb. 1962, pp. 82–88.

[9] Gaudette, R. S., del Dasal, E. P., and Crowder, P. A., "Charring Ablation Performance in Turbulent Flow," Boeing Report D2-114031-1, Sept. 1967, Boeing Co., Seattle, Wash.

[10] Georgiev, S., Hidalgo, H., and Adams, M. C., "On Ablation for the Recovery of Satellites," Research Report 47, March 1959, Avco Everett Research Lab., Everett, Mass.

[11] John, R. R. and Recesso, J., "Ablation Characteristics of a Subliming Material Using Arc Heated Air," *ARS Journal*, Vol. 29, No. 9, Sept. 1959, pp. 663–665.

[12] Vojvodich, N. S. and Pope, R. B., "The Influence of Ablation on Stagnation Region Convective Heating for Dissociated and Partially Ionized Boundary Layer Flows," *Proceedings of the 1965 Heat Transfer and Fluid Mechanics Institute*, Stanford University Press, Stanford, Calif., 1965.

[13] Winkler, E. M., Madden, M. T., Humphrey, R. L., and Koenig, J. A., "Ablation Phenomena in Supersonic Laminar and Turbulent Flows," *Proceedings of Conference on Space Simulation*, National Bureau of Standards SP-336, Oct. 1970, pp. 813–835.

[14] Rose, P. H., and Offenhartz, E., "Ablation Measurements in Turbulent Flow," Research Report 114, Aug. 1959, Avco Everett Research Lab., Everett, Mass.

[15] Comfort, E. H., "Ablation Measurements in Turbulent Flow," AIAA Paper 70-226, New York, 1970.

[16] Larson, H. K., and Mateer, G. G., "Transition Measurements on Cones in Hypersonic Flow and Preliminary Observations of Surface Ablation Grooves," BSD TR 67-213, Vol. III, Sec. 17, Aug. 1967, U.S. Air Force Ballistic Systems Div., San Bernardino, Calif.

[17] Laganelli, A. L., and Nestler, D. E., "Surface Ablation Patterns: A Phenomenology Study," *AIAA Journal*, Vol. 7, No. 7, July 1969, pp. 1319–1325.

[18] Covington, M. A., and Vojvodich, N. S., "Initial Experience With Two Arc-Heated Duct Facilities for Studying Orbital Logistic Vehicle Thermal Protection Problems," AIAA Paper 71-262, Albuquerque, N. Mex., 1971.

[19] Goldstein, H. E., "An Analytical Model for Ablation of Thoria Dispersed Nickel Chrome Alloy," AIAA Paper 71-34, New York, 1971.